Chapter

Bioethanol-Diesel Blends Used in Diesel Engines and Vehicles under Transient Operation

Octavio Armas Vergel, Dolores Cárdenas, Reyes García-Contreras and Carmen Mata

Abstract

This book chapter describes, the experiences of different experimental works related to the study of the effect of bioethanol-diesel fuel blends directly used on a study about the integrity of some parts of a diesel injection system, and on performance and regulated emissions of engines and/or vehicles under different transient conditions. The experiences described are carried out in an engine test bench, two public busses under urban transportation and a construction machine in an actual railway construction. A bioethanol-diesel fuel blend with 10% v/v of bioethanol was used for engine testing to study the potential effect on performance and emissions. Later, a blend with around 8% v/v of alcohol concentration was selected to carry out the experimental work with an injection system and with busses and construction machinery. This work points out the most important advantages and disadvantages of the use of bioethanol blended with diesel fuel. The most important strength is the potential of these fuel blends for reducing particle matter without penalty in nitrogen oxides emissions. As main weakness can be cited the need for adding a stabilizer additive which restricts the desirable increase of bioethanol content in the blend.

Keywords: diesel, engine, vehicles, transient operation, emissions

1. Introduction

The interest of using renewable fuels started at the beginning of the 21st century due mainly to: the reduction of fossil fuels consumption and the decrease of carbon footprint of the combustion products. Although biodiesel is the biofuel most widely used in compression engines, bioethanol became in a competitor since its composition presents an oxygen concentration three times higher than biodiesel. Additionally, the production cost is competitive with fossil fuel because it can be produced locally through fermentation of sugar derived from corn or cellulosic biomass [1].

Bioethanol can be used as fuel in diesel engines by means three ways:

- Dual fuel system. Apart from the traditional diesel injection system, an additional system for the injection of bioethanol is added which can be located in the intake air manifold [2] or in the cylinder but independently of the injector of diesel fuel [3, 4]. This configuration implies an additional cost but allows to work with a higher ethanol-diesel ratio.

- Fumigation. Bioethanol is atomized using a carburation in the intake air manifold and introduced together with air in the cylinder. The main advantage is that the evaporation of ethanol reduces the temperature in the cylinder (increasing the air density) could reach higher engine power [5, 6]. However, the concentration of alcohol is limited to avoid the "knocking" at high engine load and the "misfiring" at low engine load [7, 8].

- Bioethanol-diesel blends. No engine modifications are required for blends up to 30% of alcohol concentration, making bioethanol-diesel blends (named as e-diesel) the most common way to use this alcohol as fuel in compression ignition engines. The main drawbacks associated to these blends are the limited miscibility of bioethanol in diesel and their poor lubricity properties.

Reductions in terms of pollutant emissions are associated to the use of e-diesel blends. Ethanol's oxygen reduces the probability of rich-zone formation and promotes the oxidation of soot nuclei generated, reducing smoke, Particulate Matter (PM) and other pollutant emissions such as Total Hydrocarbons (THC) and Carbon Monoxide (CO). These benefits are even further than those obtained with biodiesel-diesel blends [9, 10].

The effect of e-diesel blends under steady state conditions with different ethanol concentrations has been widely studied, being the alcohol concentrations most used 5%, 7.7%, 10% and 15%. Most of the bibliography remark the reduction of smoke opacity and PM emissions with these blends [11–13]. However, real driving conditions are majority transient sequences and the effect of fuel under transient conditions could be different since the engine working characteristics are also quite different to the stationary ones. Literature related to the effect of e-diesel blends under transient operation was scarce. Giakoumis et al. [14] reviewed the effect of e-diesel (and butanol-blends) under transient operations i.e., acceleration, load increase, starting process and driving cycles, until 2013. In the introduction of this chapter, this literature is updated and enlarged with studies related to the influence of bioethanol on the durability or wear of different engine parts.

Regarding engine testing, Ahmed et al. [15] carried one of the first works out by where two e-diesel blends (with 10% and 15% of alcohol concentrations) were tested under Federal Test Procedure (FTP) transient cycle of a heavy-duty diesel engine. Reduction up to 41% of PM emissions were recorded, being the decrease proportional to the alcohol concentration, with no penalty in NOx emission (slightly decreases were obtained).

Armas et al. [16] started to evaluate the effect of bioethanol testing an E10 blend under different transient sequences. Subsequently, this research studied the effect of the same percentage of ethanol, and a butanol-diesel blend (But16) under two different engine working conditions: the starting process (under warm and hot temperatures) and reproducing the New European Driving Cycle (NEDC) [17, 18]. Tests were carried out in a test bench with a light-duty diesel engine. Reductions in smoke opacity, PM and CO emissions were reported with e-diesel blend except during the cold starting process, where the high enthalpy of vaporization and low cetane number of bioethanol favor delayed premixed combustion process, increasing PM, NOx and THC emissions under this engine working sequence although the oxygen presence in the fuel.

The aim of the study of van Niekerk et al. [19] was investigating the effect of ethanol-biodiesel-diesel blends tested over the World Harmonized Light Vehicle Test Procedure (WLTP) using an ignition compression engine. Seven binary and ternary blends were selected by means a Design of Experiments (DoE). Pollutant emissions were measured, and different statistical models were used to describe

trends obtained. Authors concluded that the ternary blend B2E9, considered as the optimum, showed reductions in CO emissions of 34%, in NOx emissions of 10% and 21% in CO_2 emissions compared to diesel.

Regarding vehicles testing, emissions tests were carried out by Randazzo et al. [20] with a light-duty vehicle positioned over a chassis dynamometer under NEDC conditions. In this work, bioethanol was added (at very low concentration, 2% and 5%) of two blends biodiesel-diesel with 20% of biodiesel concentration. Authors concluded that the use of bioethanol reduced NOx and CO_2 emissions but, surprisingly, it was unfavorable for CO, THC and PM emissions. Although the higher oxygen concentration of bioethanol (compared to biodiesel fuel), its lower cetane was considered as a factor that favored the PM emissions.

Two busses used for urban transportation were tested by Mata et al. [21] using a bioethanol-diesel blend (7.7% of alcohol) in two cities at different altitudes. Notable reductions in particle concentrations were obtained with e-diesel blend while the trend of NOx emissions depended on the altitude. The engine of other bus (a Cummins B Series) was used to evaluate the effect of two e-diesel blends (10% and 15%) under the 8-mode AVL test cycle conditions [22]. PM emissions decreased 20% and 30% with e-diesel blends but no noticeable effect on the emission of NOx and even small increases in THC and CO were observed.

Regarding non-road engines or vehicles testing (machinery), few works were found about the use of bioethanol as fuel in construction machinery vehicle. Armas et al. [23] evaluated the effect of an e-diesel blend with a 7.7% of ethanol in a vibration roller under four operation engine conditions: engine start, idle, circulation and work. Significant reductions of smoke opacity were obtained during transient engine operation.

Three non-road heavy-duty diesel engines were used in the work of Merrit et al. [24] where three e-diesel blends (E7.7, E10 and E15) were used. The FTP smoke test was reproduced, results being classified into acceleration, lugging, and peak modes. Smoke and particulate matter emissions decreased (up to 20%) as ethanol concentration increased. CO emissions were also lower than those of diesel base fuel while NOx concentration was similar.

As it was commented previously, the main drawback of e-diesel blends is the limited miscibility of both fuels which requires knowing conditions where these blends are stable. Bioethanol's miscibility in diesel mainly depends on three parameters: water content (hydrous ethanol), temperature and ethanol concentration [25]. The presence of water in ethanol, the low temperatures and the high ethanol concentration difficult the miscibility between both hydrocarbons [25–27].

To ensure the miscibility between bioethanol and diesel, especially at low temperatures, different additives are usually added: alcohols (butanol, pentanol, octanol, dodecanol) [28, 29], ethers, and different co-solvents [26, 30] or emulsifiers [31, 32] whose composition is, sometimes, not published. One of the most common additives for bioethanol-diesel blends is biodiesel fuel which, in addition to its renewable origin, contributes to improve the cetane number and lubricity of e-diesel blends [33, 34]. Different authors evaluated the stability of bioethanol-biodiesel-diesel (named as e-b-diesel) blends at different temperatures, indicating the different instability areas [9, 35].

Apart from the limited miscibility, easily resolved by the incorporation of additives, the poor lubricity properties of bioethanol could imply wear of the fuel injection system and other engine components. Two types of investigations have been carried out in relation to this topic:

- Wear of metallic materials. Wear Scar Mean Diameter (WSMD) of different e-diesel and e-b-diesel blends was evaluated in the work of Lapuerta et al. [36].

The increase of WSMD was not linear with the increase of ethanol concentration. Durability tests of fuel injection system using several experimental techniques were carried out by Armas et al. [37]. A E7.7 blend showed similar effect on durability of the injection pump parts than that the diesel fuel but a reduction (around 20%) of nozzle hole effective sections was produced with the blend. In the rest of literature, wear of the injection system parts with bioethanol-diesel blends is observed [38, 39].

- Material degradation/oxidation. Some metals (zinc, plumb, copper, aluminum) and some plastics (rubber and polyvinylchloride, PVC) are oxidized when contacting with bioethanol [40]. To solve this drawback, some authors suggest the use of stainless steel as a substitute for metals (aluminum, magnesium and brass) [41, 42] and, in other work, high-density polyethylene is used instead of rubber or other plastic materials in [40].

The aim of this chapter is to show the main results of several works about the effect of bioethanol-diesel blends on the durability of fuel injection system and on the performance and emissions in diesel engines or vehicles under transient working conditions.

2. Experimental installations, procedures and fuel blends characteristics

2.1 Engine testing

With the objective to evaluate the effects of bioethanol blended with diesel fuel, under transient operation, previously to the direct use in vehicles, an experimental study with an engine mounted on a test bench is recommendable. In this case, **Figure 1** shows a general sketch of the experimental installation used for testing the engine under discrete transient sequences. A turbocharged intercooled, direct injection Diesel engine, 4-cylinder, 4-stroke, typically equipped in European light duty vehicles, was employed as experimental unit. In **Table 1**, main characteristics of the engine tested are listed.

The engine was coupled to an asynchronous machine Schenck Dynas3 LI 250 (operating as a dynamometer). The dynamometer control system allowed measuring, controlling, and registering the engine speed, accelerator position and effective

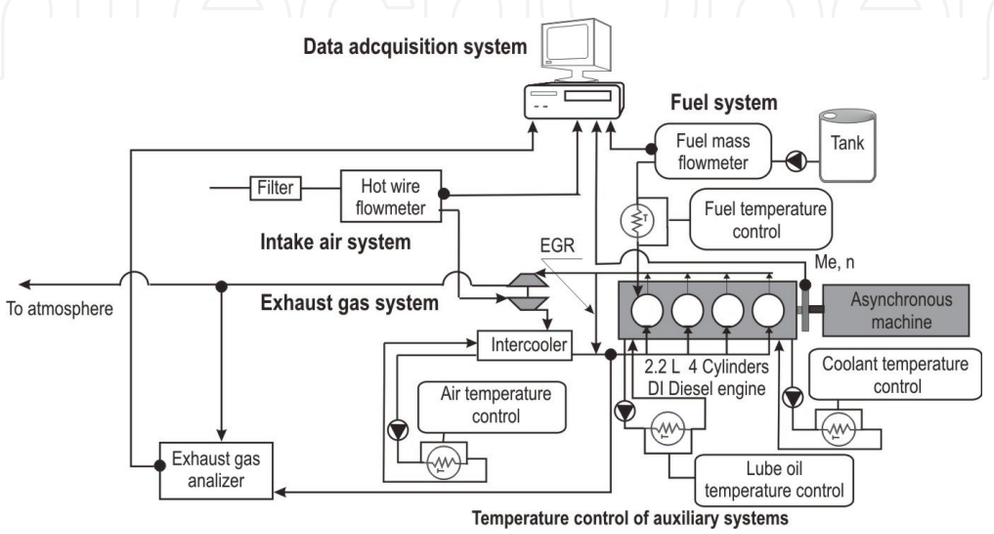

Figure 1.
Sketch of the experimental installation for engine testing.

Parameter	Value
Compression ratio	18:1
Swept volume (L)	2.2
Stroke (m)	0.94
Bore (m)	0.865
Cylinders arrangement	4, in line
Maximum rated torque (at 2000 min^{-1}) (Nm)	237.4
Maximum rated power (at 4000 min^{-1}) (kW)	85.2 kW
Fuel injection system	VP44 pump, electronically controlled
Main injection pressures (bar) at full load (at 2000 min^{-1}) at idle (750 min^{-1})	1100 200

Table 1.
Main characteristics of the engine tested.

torque. Instantaneous fuel consumption was registered by means of a PLU 401/116H flow meter, while the air mass flow rate was measured by means of a hot-wire flow meter Siemens 5WK9628, previously calibrated in the 0–718 kg/h range with an accuracy of 2% around the measured value.

The Exhaust Gas Recirculation (EGR) ratio was calculated by comparison of the CO_2 gas concentration at the inlet and at the exhaust manifolds using an infrared absorption gas analyzer Environnement MIR2*M. NOx* emissions were measured by means of a chemiluminescence analyzer Environnement TOPAZE. In both cases (CO_2 and NOx) the acquisition frequency was 3 Hz. The smoke opacity of the exhaust gas (as characteristic parameter of particulate matter emission) is proportional to the total light extinction across the exhaust gas stream. Using a partial flow opacimeter AVL 439 with a frequency of 10 Hz, the smoke opacity was registered. Instantaneous engine parameters were registered by means of a Yokogawa OR1400 data acquisition system. This system has the possibility for data registering in a range from 1 Hz to 100 kHz. Finally, the sampling frequency of gaseous emissions, test bench parameters and the smoke opacity was 10 Hz.

For assessing the effect of changes in engine load on the smoke opacity and NOx emissions, two discrete transient sequences were tested and compared. In each sequence both, the initial and final conditions of effective torque and engine speed, were the same independently of the fuel tested.

Figure 2 shows these two transient sequences, both with effective torque (Me) increase at relative low engine speed (n) and denoted as A_M-A_F and A-A'. The aim of this methodology was to evaluate the smoke opacity and NOx emissions behavior under two of the most common transient sequences with fuel consumption demand in any type of vehicles. Under A_M-A_F sequence, the engine was driven from motored to fired conditions. This test tries to simulate a vehicle acceleration from zero fuel delivery to a given load condition. Meanwhile A-A' is the typical transient sequence with load increase at constant speed (for example, under a slope positive change in a road profile, remaining constant the vehicle velocity without gear changes). Under both cases, the engine control unit (ECU), tuned by manufacturer, controlled the EGR valve opening.

Initial and final operating modes of the sequences shown in **Figure 2** and **Table 2** were chosen due to their operation representativeness of that zone on the engine torque-engine speed map (under low load and engine speed) where the pollutant emissions restrictions are very important (typical of urban driving conditions).

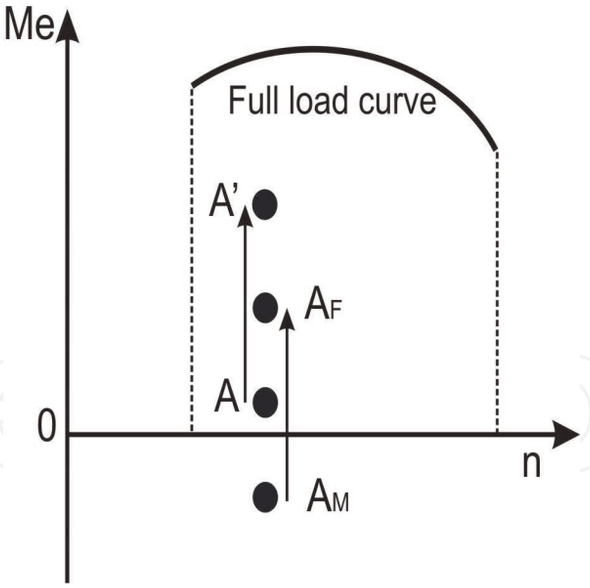

Figure 2.
Engine transient sequences tested.

Transient sequence	Engine speed (min^{-1})	Effective torque (Nm)	
		Start	End
A_m-A_f	1661	−40	55
A-A'		26	90

Table 2.
Steady state operating conditions before and after each transient sequence.

Under engine transient testing, a low Sulfur diesel fuel was used as reference (denoted as Ref). A 10% v/v blend of bioethanol with this diesel fuel, without stabilizing additive, was denoted as E10. This blend was selected because the ambient temperature was higher than 25°C. Under these thermal conditions and, during relative short time period, the blend is stable without additive since Bioethanol used has a purity of 99.94%. The bioethanol concentration of the tested blend was defined attending to the results of previous studies [26]. The main properties, either measured or calculated, of the tested fuels are presented in **Table 3**.

2.2 Parts durability testing

Before the extension of the work for assessing the benefits of bioethanol-diesel blends in vehicle captive fleets, two works must be done: a study about the miscibility and stability of the blends with different bioethanol concentrations [26] and the study of the effect of the fuel blend on the integrity of some parts of the engine injection system [37]. Both works are essential for verifying the lubricant capacity of the fuel blend under real driving conditions. This sub-section describes, as example, part of the work done with some pieces of a modern injection system.

The experimental unit used was a Bosch high-pressure injection pump. Normally this pump operates connected to a common rail and this one connected to a fuel injector, electronically controlled. This model of experimental unit equips great number of different models of Mercedes Benz light duty cars. This system also equips great part of diesel engines, with around 2 liters of cylinder displacement, commercialized in Europe. The main characteristics of the injection system studied in this work are shown in **Table 4**.

Property	Fuel		
	Ref	E10	E
Density (kg/m^3)[a]	833.5	828	792
Kinematic viscosity (cSt)[b]	2.79	2.13	1.13
Gross heating value (MJ/kg)	45.89	43.48	28.05
Low heating value (MJ/kg)[c]	42.84	40.44	25.18
Low heating value (MJ/L)[c]	35.70	33.49	19.94
% C (in weight)	85.23	82.08	52.17
% H (in weight)	13.92	13.83	13.04
% O (in weight)	0.74	3.98	34.78
% S (in weight)	0.026	0.024	0
Molecular weight	206.9[d]	155.2[e]	46.06[e]
Stoichiometric fuel-air ratio[e]	1/14.60	1/14.07	1/9.01
Distillation			
Initial Boiling Point (°C)	182	78	78
T10 (°C)	204	79	
T50 (°C)	266	257	
T90 (°C)	348	347	

[a]*Measured at 15 °C.*
[b]*Measured at 40°C.*
[c]*Calculated from composition and gross heating value.*
[d]*Calculated with software Aspen-Advisor.*
[e]*Calculated from composition.*

Table 3.
Fuel properties used under engine testing.

Injection system characteristic	Value (unit) and/or information
Pump manufacturer	Bosch
Pump type	first generation with pistons
Common rail model	270 CDI MB/4 injectors
Common rail length (m)	0.55
Pump-common rail line length (m)	0.40
Common rail-injector line length (m)	0.15
Inner diameter of lines (m)	0.002

Table 4.
Main characteristics of the injection system tested.

Figure 3 shows the scheme of the hydraulic circuit of the experimental installation used for simulating a long-term work of an injection system under demanding operating mode. The injection system worked on an injection test bench (model Asia Diesel). In dark black, the circuit (without modifications) for testing diesel fuel is presented. Those parts modified for testing bioethanol-diesel blends are presented in light gray (valve 2 and tank caps). Those parts were added to remain the water content in the range established by the European fuel quality standard EN-590 and for avoiding the ethanol evaporation to the atmosphere. In addition,

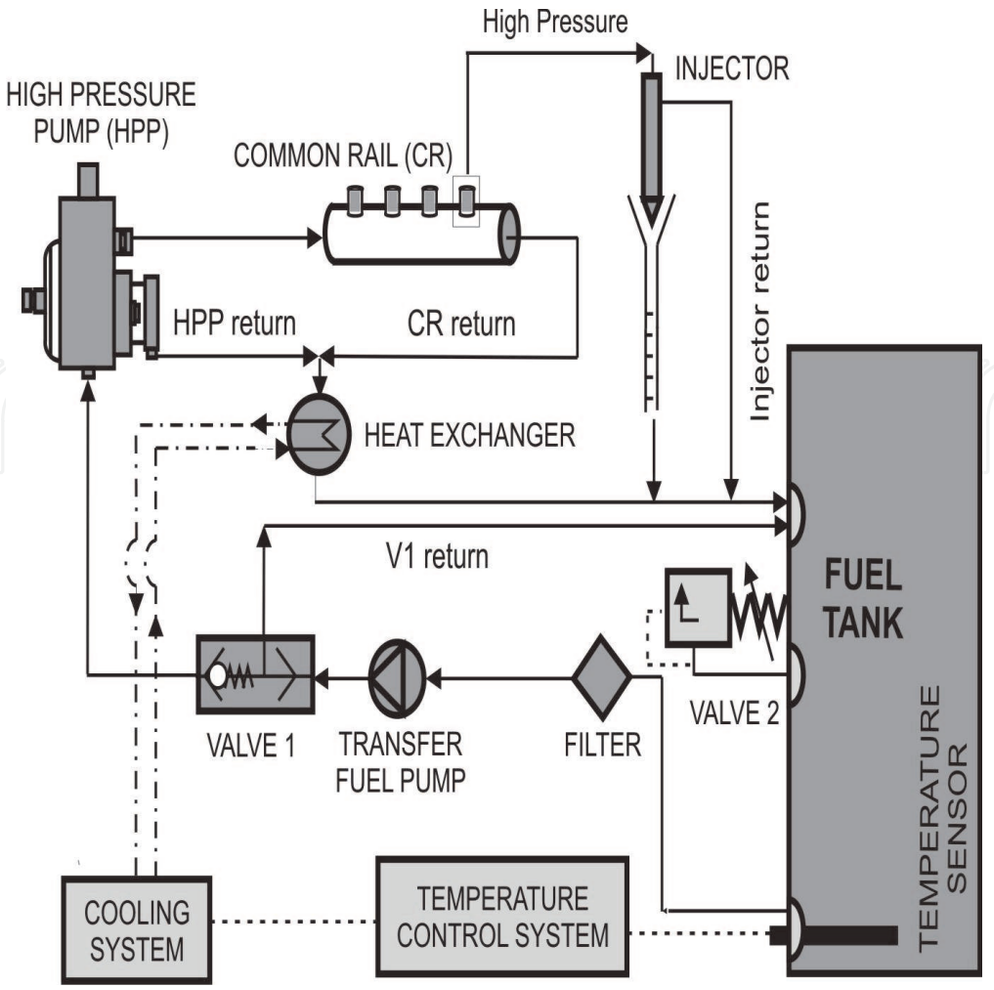

Figure 3.
Scheme of the hydraulic circuit of the test bench for simulating long-term work with fuels tested.

the fuel tank was instrumented with a pressure and/or vacuum safety valve, to prevent the pressure variation inside the fuel tank. These modifications were also needed in the fuel tanks of the vehicles tested.

Table 5 shows the test conditions for simulating reproduced by the test bench during the long-term work of a new injection system used with each fuel tested.

Before and after the long-term operation with each fuel, the total fuel delivery was determined using diesel fuel and those conditions presented in **Table 5**. Selected test conditions (600 work hours at 2500 min^{-1} and 1500 bar of injection pressure) are equivalent to the driving of a light duty vehicle during more than 120,000 km.

For characterizing, the effect of fuels on the integrity of some parts of the injection system, different techniques can be used. Among these techniques are the

Parameter	Unit	Value
Rotation speed	min^{-1}	2500
Injection pressure	bar	1500
Injection time	ms	1
Fuel temperature	°C	40
Operation time	hours/day	10–12
Total test time	hours	600

Table 5.
Test conditions for simulating reproduced by the test bench.

following: measurement of the fuel delivery, characterization of the roughness surface of elements, observation of the surface microstructure, weigh of elements and measurement of the nozzle geometry inner shape obtained by casting silicone, determined from images of a Scanning Electronic Microscope (SEM). In this chapter, the effect of E8 fuel blend on the surface roughness of the drive shaft of the fuel high-pressure pump (**Figure 4a**, surfaces Ds1, Ds2 and Ds3), the geometry of the nozzle (**Figure 4b**, diameters along the nozzle hole in three positions d1, d2, d3) and the total fuel delivery is compared. Comparison was done, before and after 600 work hours, with diesel fuel.

For determining the effect of the long-term work on the surface roughness a tester Hommel Werke, model T500, was used. This tester has capacity to determine different parameters of surface roughness, along 10 mm of the sampled surface, with 100 microns amplitude and with a precision of 0.01 μm. Diameters along the nozzle hole were determined from images obtained by means of a scanning electronic microscope Philips model XL30 of the hole inner shape obtained by casting silicone [43].

This part of the work and the work done with both busses and with construction machine, as will be explain later, was carried out with a different bioethanol-diesel fuel blend. In these two cases, a low Sulfur diesel fuel was used as reference (denoted as Ref). A 7.7% v/v bioethanol-fuel blend, with 0.62% v/v of a confidential stabilizing additive, was used and denoted as E8. **Table 6** shows properties of fuels used in this part of the work. Bioethanol purity was 99.94%. Since the additive composition was not known, all E8 fuel characteristics, dependent on the fuel composition, were determined only from diesel and bioethanol fuels.

2.3 Vehicle testing. Urban busses

Two similar busses used for urban transportation were tested. One of the vehicles was a Euro II IVECO Europolis 915 city bus (denoted as IV), around 10 T in weight, equipped with a 6-cylinder, with around 6 L of displacement, direct injection, turbocharged, heavy-duty diesel engine. This bus was equipped with an automatic ZF transmission. The bus length is 9 m. The other vehicle was a Euro II Renault city bus (denoted as RE), around 13 T in weight, equipped with a 6-cylinder, with around 8 L of displacement, also turbocharged, direct injection, heavy-duty diesel engine. This bus was equipped with an automatic Voith transmission and its length is 10 m. Both busses were equipped with injection systems including injection pumps electronically controlled. Both busses operate with single

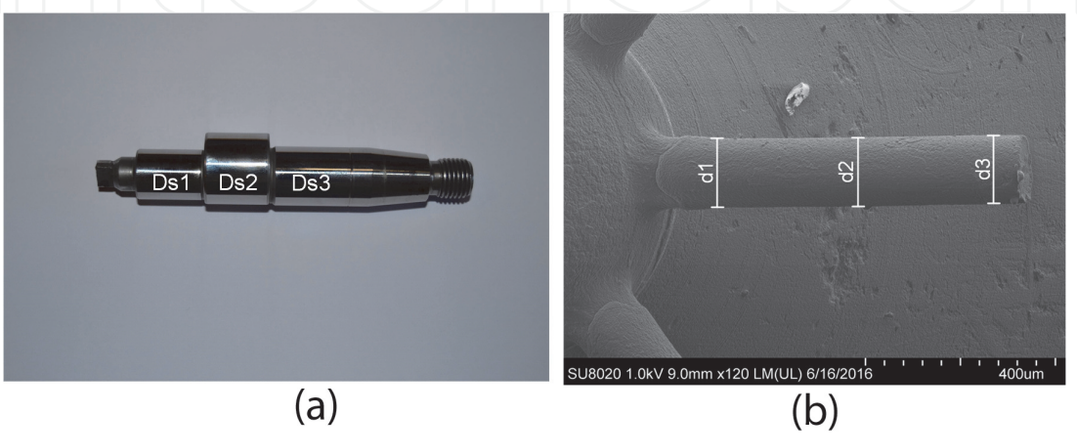

Figure 4.
a) Surfaces of the drive shaft of the high-pressure pump studied and (b) example of a SEM image from the silicone mold of a hole of the injector nozzle.

Property	Fuel		
	Ref	E8	E
Density (kg/m^3)[a]	834.9	831	792
Kinematic viscosity (cSt)[b]	2.72	2.41	1.13
Gross heating value (MJ/kg)	45.54	43.82	28.05
Low heating value (MJ/kg)[c]	42.58	40.86	25.22
Low heating value (MJ/L)[c]	35.55	33.95	19.97
% C (in weight)	86.13	83.63	52.14
% H (in weight)	13.87	13.82	13.13
% O (in weight)	0	2.55	34.73
% S (in weight)	0.0034	0	0
Molecular weight	211.7[d]	167.5[e]	46.06[e]
Stoichiometric fuel-air ratio[e]	1/14.67	1/14.25	1/9.00
Distillation			
Initial boiling point (°C)	172	78	78
T10 (°C)	211	178	
T50 (°C)	270	256	
T90 (°C)	340	337	

[a]*Measured at 15 °C.*
[b]*Measured at 40°C.*
[c]*Calculated from composition and gross heating value.*
[d]*Calculated with software Aspen-Advisor.*
[e]*Calculated from composition.*

Table 6.
Properties of fuels used in parts durability testing and in busses and construction machinery testing.

injection and advanced Start of Injection (SoI) and without Exhaust Gas Recirculation (EGR). Both vehicles, with similar mileage, were not equipped with after-treatment devices (Diesel Oxidizer Catalyst (DOC) nor Diesel Particulate Filter (DPF)). This configuration of the exhaust systems allowed studying the effect of fuels on pollutant emissions without influence of after-treatment devices.

As **Figure 5** shows, both busses and the construction machine were instrumented with a HORIBA OBS 1300 gas analyzer and with a TSI Engine Exhaust Particle Sizer (EEPS) spectrometer. The first of them includes sensors for measuring and registering the relative fuel-air ratio and ambient conditions (temperature, pressure and humidity). In both cases, vehicle velocity and its position were determined by means of a Global Positioning System (GPS) and an inertial sensor. Although the HORIBA OBS 1300 includes different measurement modules, only the MEXA 720 NOx with a zirconia sensor for nitrogen oxides measuring was used. For characterizing particulate matter, an EEPS spectrometer was used to measure particle size distributions under transient vehicle operation. **Figure 5** also shows, the EEPS spectrometer coupled to a Rotating Disk (RD) diluter model MD19-2E, as primary dilutor, and an air supply-thermal conditioner model ASET15–1 with an evaporating tube, as secondary dilutor.

At Ciudad Real city, the tests were carried out in a route with 14.5 km length (around one hour in time). This route mostly runs throughout the city center, characterized by a low mean velocity. However, it includes some stretches of

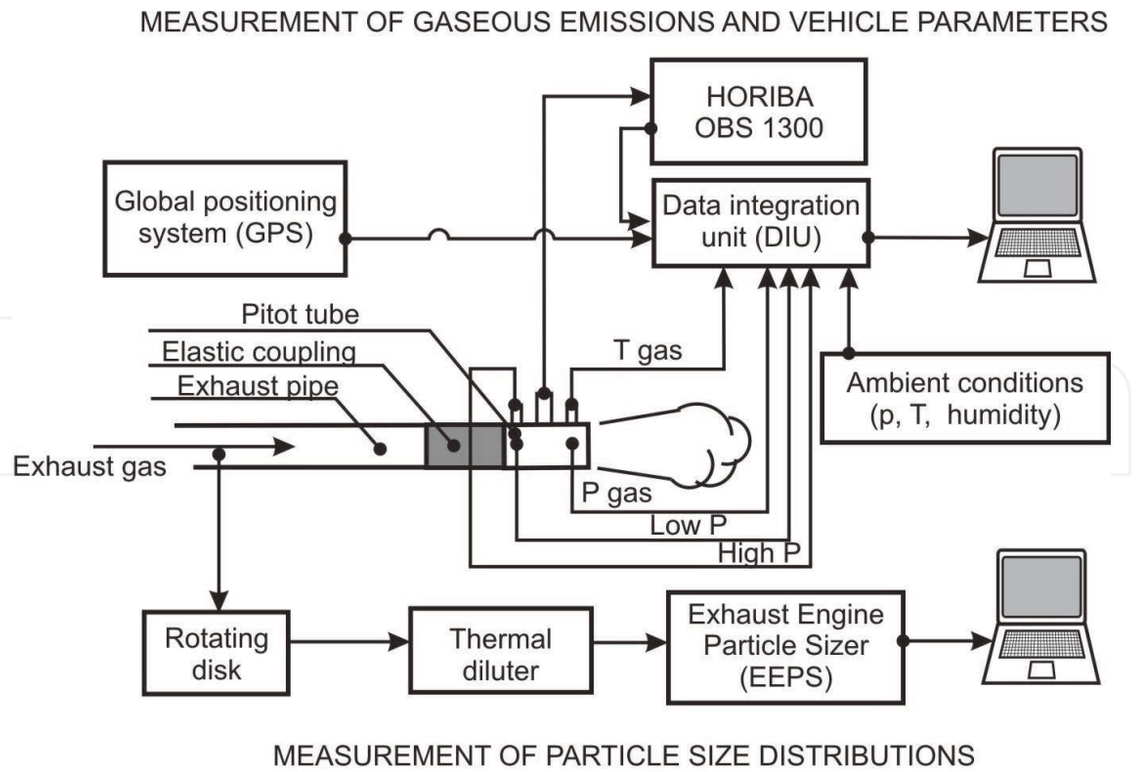

Figure 5.
Sketch of the experimental installation for vehicle testing (busses and construction machine).

medium speed (around 50 km/h). The altitude profile is almost constant during the entire route (~650 m above the sea mean level). The route has 67 stops for passengers, uniformly distributed along the trajectory and it includes 31 traffic lights.

At Sevilla city, the tests were carried out in route with 13 km length (also one hour in time). The route runs mostly throughout the city center with similar mean velocity as occurred at Ciudad Real city. The altitude profile is almost constant during the entire route (~10 m over the sea level). The route has 35 stops for passengers, uniformly distributed along the trajectory and it includes 21 traffic lights.

The comparison of the results obtained from real driving operation of test vehicles is relatively complex. By this reason, results presented in this chapter were processed following the methodology presented in [44]. In this case, comparison between busses and fuels, based on the obtained mean values from categories, will be presented below. Cycle is the whole data from the beginning to the end of the route while category is that part of the cycle with similar variation of the most important operating parameters (relative fuel-air ratio, denoted as Fr and vehicle velocity, denoted as Vv).

A great number of different categories such as accelerations, decelerations, idle, etc. composes one cycle [44]. In this text only the analysis of part of the events included within the acceleration category is presented. Within the acceleration category, there are three possible situations: a) acceleration coming from idle, b) acceleration coming from deceleration without fuel consumption and c) acceleration coming from deceleration with fuel consumption. As example, **Figure 6** shows vehicle velocity and fuel-air ratio profiles, registered during part of a cycle.

Four categories, idle (I), acceleration (A), deceleration with fuel consumption (DwF) and deceleration without fuel consumption (D) [21] were selected as example for this work. In this chapter, as example, only the comparison under acceleration coming from idle sequence is presented.

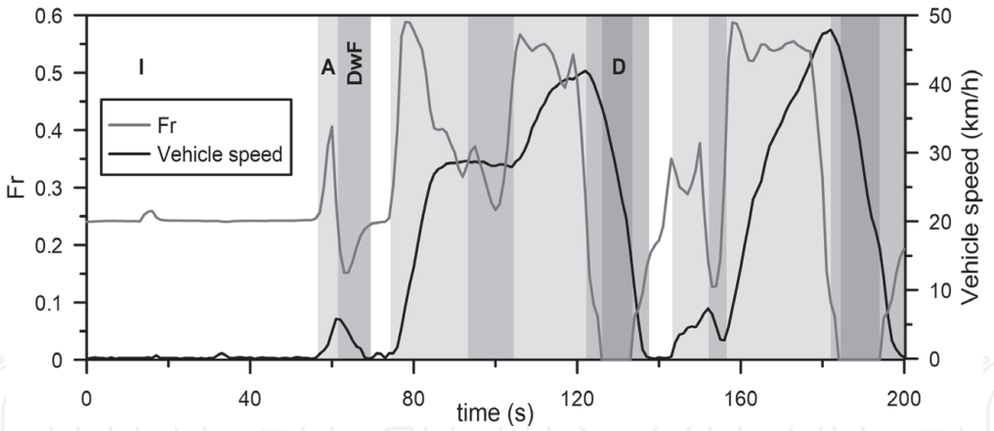

Figure 6.
Vehicle velocity and relative fuel-air ratio profiles from part of the bus cycle.

2.4 Vehicle testing. Construction machinery

As experimental unit was used a vibrating roller Lebrero model Rahile 155TT. This machine equips a direct injection Diesel engine, 6-cylinder, 4-stroke turbocharged, typically used during roads and railways construction. **Table 7** shows the most important characteristics of its engine.

This machine was instrumented with a HORIBA OBS 1300 system as **Figure 7** shows. Its connection to the exhaust pipe was similar to that used in public busses. However, the smoke opacity (indicative of the particulate matter emitted), which ranges from zero to 100% and proportional to the total light extinction across the exhaust gas stream, was determined by a smoke opacimeter Wager 6500. This signal was also registered by the OBS system.

The comparative analysis of pollutant emissions registered under the operation of a construction machine is complex. As occurred with public busses and regarding the engine work, the work done by the machine can be classified into five categories [23]. These categories are engine start on (denoted as S), idle (denoted as I), circulation (denoted as C) and work (denoted as W).

This categorization allows the daily machine operation without disturbance on its own work. This machine, during the tests, worked under real operating conditions during the construction of a railway. The best option is to register engine parameters and pollutant emissions in different occasions during the selected

Parameter	Value
Model	Deutz FL6913 turbocharged
Rated power highly intermittent at 2500 min^{-1} (kW)	109
Rated torque at 1700 min^{-1} (Nm)	510
Compression ratio	15.5:1
Displacement (L)	6.128
Cylinder arrangement	6, in line
Bore (m)	0.102
Stroke (m)	0.125
Fuel injection system	Bosch in line injection pump

Table 7.
Main engine characteristics of the construction machine.

Figure 7.
View of the experimental installation located on the construction machine.

operation sequences. In result and discussion section, results related to C and W sequences are presented as example.

3. Results

3.1 Engine testing

Time evolution of the smoke opacity (characteristic parameter of particulate matter emission) and NOx concentration, under transient sequence A_M-A_F, is presented in **Figure 8**. This behavior can be explained because both relative fuel-air and EGR ratios were zero at the beginning of the transition avoiding, this way, soot depositions on the internal of the manifold walls and thus any further blowing effect. Great reduction of smoke opacity is observed when E10 blend is used compared to reference fuel. The increase of the oxygen content of the fuel blend and the reduction of the aromatic content explain this result. Additionally, as **Figure 9** shows, the EGR ratio at the end of the transient sequence with the E10 blend, would hardly reach that of reference fuel. This also would leads to a greater availability of oxygen at the end of the transition, contributing to the smoke opacity reduction registered.

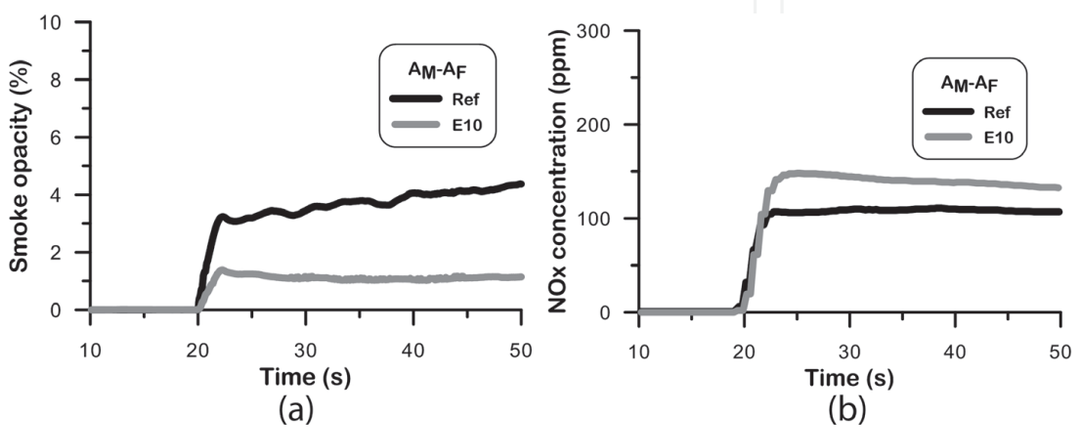

Figure 8.
Time evolution of the smoke opacity (a) and NOx concentration (b) during the A_M-A_F transition.

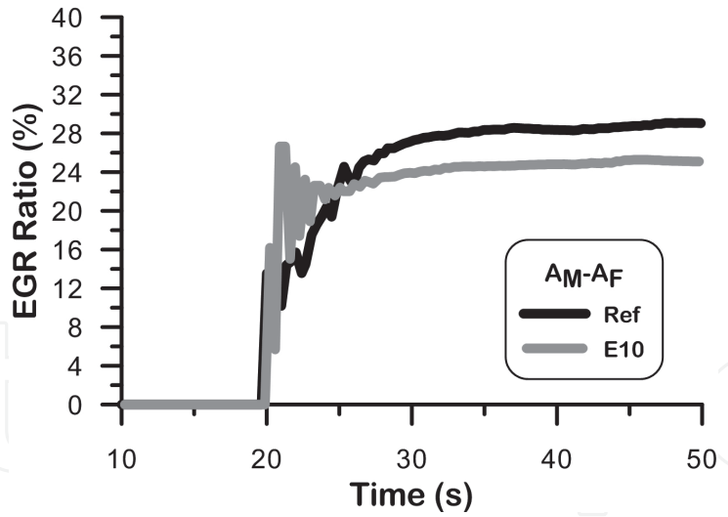

Figure 9.
Time evolution of EGR ratio during the A_M-A_F transition.

However, the slight increase of NOx concentration registered along the transition with E10 blend (see **Figure 8b**) can be explained by the initial oscillations of the EGR ratio (due to the sensibility of the EGR valve opening) presented in **Figure 9**. It is important to take into account two factors: i) manufacturer tuned the engine (included the EGR valve opening) with diesel fuel and ii) under a typical diesel combustion process, increases in EGR ratio generally produce decreases of NOx concentration but increases of smoke opacity, this last as characteristic parameter of particulate matter.

Figure 10 presents the smoke opacity and NOx concentration time evolution along the transition A-A' registered with both fuels. As **Figure 10** shows, the shape of the smoke opacity and NOx concentration curves during their time evolution are similar between both fuels.

This shape is consistent with the shape of the relative fuel-air ratio (related to the stoichiometric fuel-air ratio) and EGR ratios as **Figure 11** presents.

In this figure, as example, is presented the time evolution of both parameters registered with both fuels. It is important to remember that the engine is forced to reach the same torque value at the beginning and at the end of the transition.

The sudden increase of the relative fuel-air ratio is caused by the delayed response of the turbocharger. As consequence, this produces a time lag between the fresh inlet airflow and the increase of fuel delivery demanded to reach the torque target at the end of transition. Additionally, other contributor factor of the smoke

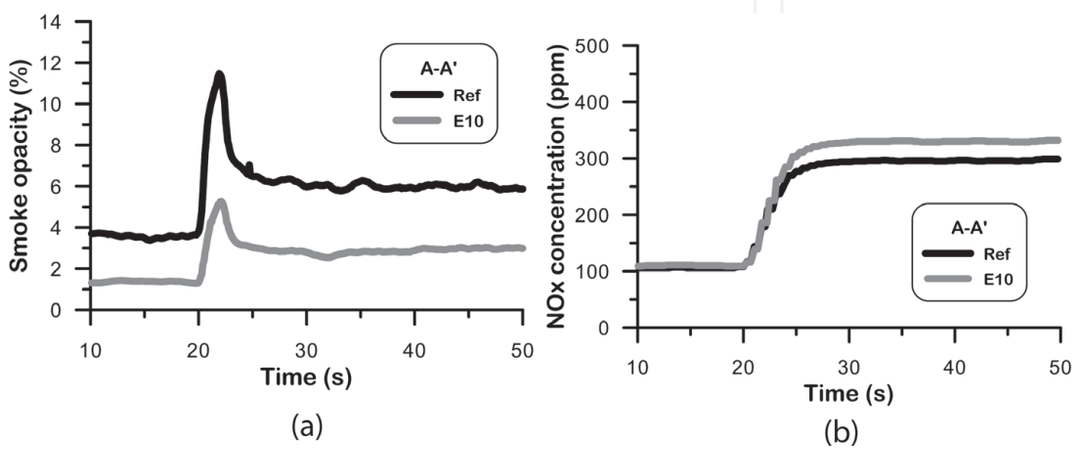

Figure 10.
Time evolution of the smoke opacity (a) and NOx concentration (b) during the A-A' transition.

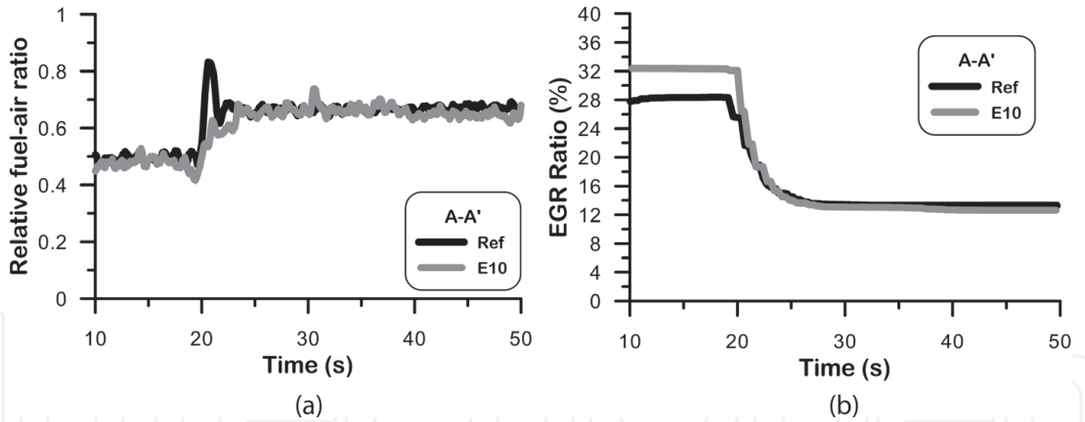

Figure 11.
Time evolution of relative fuel-air ratio (a) and EGR ratio (b) during the A-A' transition.

opacity peaks is the release of soot deposited on the pipe walls during the steady operation previously to the transition, which could be blown out as consequence of the increased exhaust gas flow with higher thermal conditions.

As can be seen in **Figure 10a**, the smoke opacity is clearly lower with E10 blend. The lower viscosity and higher volatility of E10 fuel could favor the fuel spray atomization and its evaporation, just during the transition. Effectively, the reduced content of aromatic compounds and the higher oxygen content of the E10 blend follows being the most important contribution to the reduced smoke peak.

Regarding NOx concentration presented in **Figures 8b** and **10b**, different properties of the bioethanol-blend cause opposite effects on this pollutant emission. First, the low adiabatic flame temperature and the high vaporization heat of the E10 blend reduce the combustion temperature and the NO formation [45]. Second, a low cetane number (leading to longer delay time), the high oxygen content, a fast combustion velocity and an advanced fuel injection (this being a response of the control unit for compensating the longer injection process due to the reduced heating value), are those factors which favor high combustion temperature and NO formation [45–48]. According to these two groups of factors and depending on the engine operating mode and the type of engine both increases and decreases of NOx with bioethanol-diesel blends have been reported [45–48].

These results indicate the great potential to obtain important reductions of smoke opacity without penalty of NOx emissions by tuning the engine with a bioethanol-diesel blend.

3.2 Parts durability testing

For the surface roughness analysis, two parameters were used: the arithmetic mean roughness value (Ra) and the mean peak to valley height (Rz), both defined by the DIN4777 and ISO4287 standards. The mean roughness (Ra) is defined as the arithmetic mean of the profile deviation of the filtered roughness profile from the mean line (ML) within the measuring length (L), according to Eqs. (1) and (2) and the representation shown in **Figure 12**.

$$R_a = \frac{1}{L}\int_0^L |y| dx \tag{1}$$

$$R_a = \frac{\sum^i Areas\ A_i + \sum^j Areas\ A_j}{L} \tag{2}$$

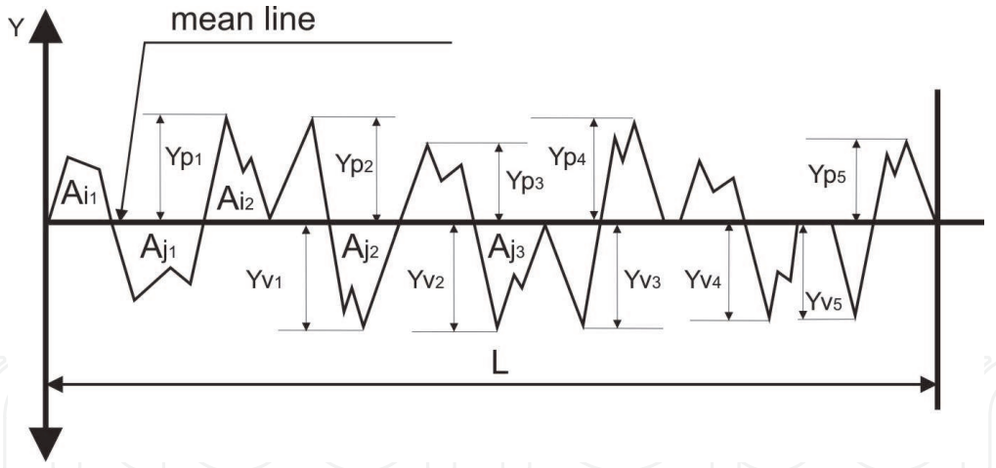

Figure 12.
Sketch of the surface roughness with peaks and valleys.

The mean peak to valley height (Rz) is defined as arithmetic mean from the peak to valley heights y_1 to y_5 of five successive sampling lengths in the filtered roughness profile, according to Eq. (3).

$$R_z = \frac{\sum_{i=1}^{i=5} y_{p_i} + \sum_{j=1}^{j=5} y_{v_j}}{5} \tag{3}$$

The absolute differences ΔRa and ΔRz were calculated by means of the Eqs. (4) and (5) in order to determine the effect on surface roughness of each fuel tested before and after of the long-term work. These differences were obtained between the final and initial mean values of the Ra and Rz parameters of each zone of the drive shaft shown in **Figure 4a**.

$$\Delta Ra = Ra(600h) - Ra(0h) \tag{4}$$

$$\Delta Rz = Rz(600h) - Rz(0h) \tag{5}$$

Ra and Rz parameters measured on the drive shaft surfaces Ds1, Ds2 and Ds3, with both fuels, are presented in **Figure 4a**. In addition, the 95% confidence interval using three measurements at each point is indicated. According to the results presented in **Figure 13**, the greatest Ra and Rz parameters values were calculated in that surface denoted as Ds3 and this occurred independently of the fuel tested.

The surface roughness measured on this zone was more pronounced than those measured on Ds1 and Ds2 surfaces were. The zone Ds3 is located on the most loaded section surface of the drive shaft. The measured surface roughness fits in the grade N4 to N2 (N is the surface finish grade as per the standard ISO1302). This classification corresponds to machined surfaces derived from lapping and/or finishing turning operations. It is important to highlight that if the surface roughness of two contact surfaces drastically decreases (below 0.025 mm), it could lead to the blockage of the elements due to surface adherence (lapping effect). In the surface Ds3), the flange transmits a great force to the drive shaft, and this action leads to a high friction value. The values calculated of the parameters Ra and Rz for the surfaces Ds1, Ds2 and Ds3 were similar, prior to and after the durability test, independently of the type of fuel used. **Figure 14** shows the maximum ΔRa and ΔRz values that were measured on each point along the drive shaft.

Results presented in **Figures 13** and **14** indicate similar effect of both fuels tested along the drive shaft. The lower lubricity of the E8 fuel blend produces a negligible effect on the surface under a long-term work equivalent to more than 120,000 km.

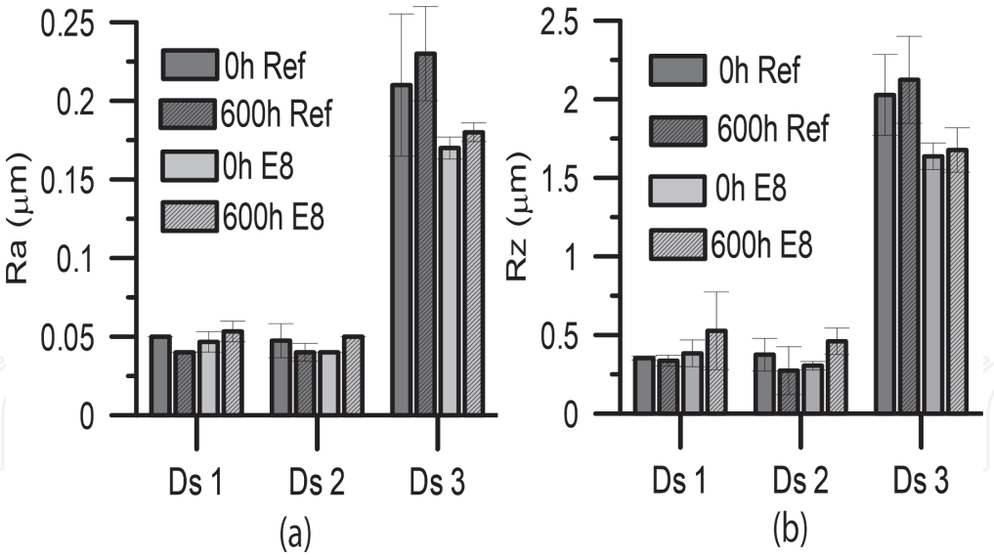

Figure 13.
Ra and Rz parameters calculated for surfaces Ds1, Ds2 and Ds3 of the drive shaft.

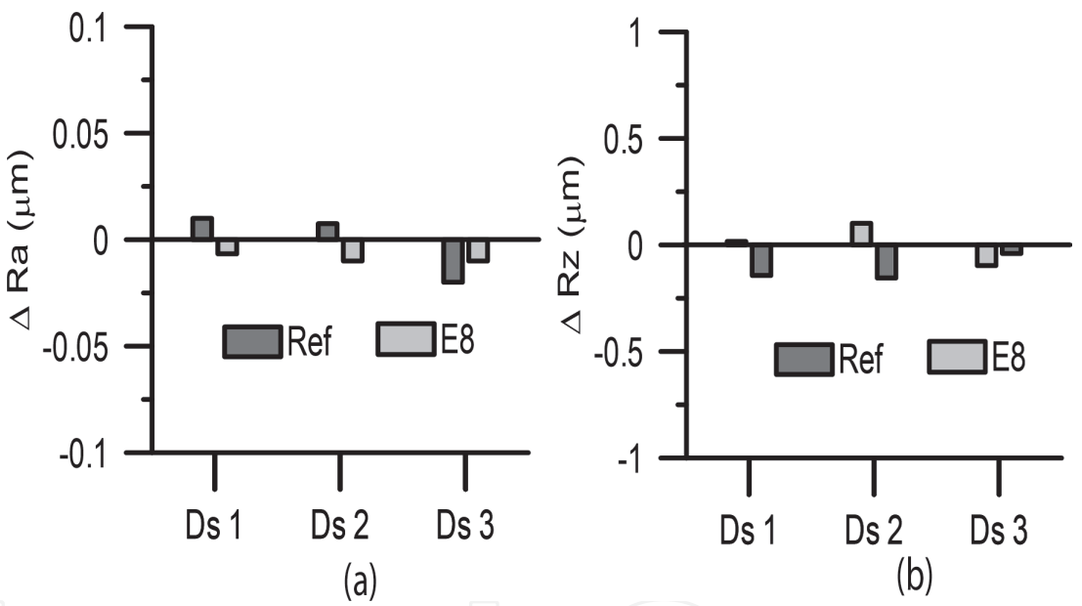

Figure 14.
Maximum ΔRa (a) and ΔRz (b) values determined from each surface of the drive shaft.

Table 8 presents diameters (d1, d2 and d3) measured from the silicone casting images taken from two randomly selected nozzle holes used with each fuel, before and after the tests. This table also shows the relative difference (ΔAd) of the

Fuel	Hole	d_A (μm) (600 h)			Mean d_A (μm)	d_B (μm) (o h)			Mean d_B (μm)	ΔAd (%)
		d_1	d_2	d_3		d_1	d_2	d_3		
Ref	1	192.8	192.8	193.0	192.9	192.8	192.8	193.1	192.9	0
	2	193.0	192.8	193.2	193.0	192.8	192.7	193.0	192.8	−0.2
E8	1	200.7	200.6	199.8	200.4	175.4	182.0	184.0	180.5	−18.9
	2	201.9	200.9	202.9	201.6	172.5	178.2	179.3	176.7	−23.2

Table 8.
Geometrical characterization of sections of nozzle holes.

effective sections (A) before (denoted as B) and after (denoted as A) the tests, calculated from mean diameters d_B and d_A, respectively.

Differences obtained, section by section, among diameters of a same nozzle used with each fuel is lower than 1.5%. This value is within the dispersion range of Bosch nozzles. Reductions of the effective sections of 18.9% and 23.2% respectively were obtained after using E8 fuel blend. These reductions can be explained by a probable sedimentation and/or oxidation along nozzle holes. This explanation could be justified because of the test bench was not completely hermetic. This situation provoked a slight reduction of ethanol concentration (around 0.2% v/v). Additionally, the water concentration increased in the blend from 243 ppm to 460 ppm, after 600 h. After the test, the experimental installation was checked. One point without a correct sealed was detected: the nozzle tip. This fact could produce the contact between the ambient air with the nozzle tip. The air oxygen could produce a slight oxidation along the holes, causing the reduction of their effective sections (**Table 9**).

The total fuel delivery determined before and after the tests with each fuel is shown in **Table 10**. This parameter varied within a narrow range of variation (around 3%), before and after the long-term work with diesel fuel. Contrary, the total fuel delivery decreased approximately 30% after the test with E8 fuel blend.

3.3 Vehicle testing. Urban busses

In this section, the time analysis of acceleration sequences (A) registered through the test cycles is presented. This analysis has been carried out by comparison of five seconds of those sequences with similar time profiles of the relative fuel-air ratio (Fr). **Figure 15** presents the average time evolution of Fr, Vv, NOx concentration and its mass flow rate from both busses and fuels tested respectively.

As can be seen in **Figure 15**, the Fr profiles between vehicles and fuels were similar enough for comparing the effects of fuels. NOx concentrations from E8 fuel were lower compared to diesel fuel when the IV bus was tested, and it was higher when the RE bus was tested. In both cases, the difference between average NOx concentrations produced by fuels, in both vehicles, was practically constant along the sequence.

Fuel	Fuel delivery (cm^3 per stroke)		
	Before	After	Relative difference %
Ref	6.0	6.2	+3
E8	6.1	4.3	−29.5

Table 9.
Total fuel delivery before and after the tests with both fuels.

Sequence	Parameter						
	Fuel	Fr	T_{amb} (°C)	T_{exh} (°C)	$\dot{V}_g$ (L/min)	$\dot{m}_{fuel}$ (g/s)	υ (km/h)
C	Ref	0.308	9	243	5444	1.221	7.6
	E8	0.312	0	238	4025	0.950	6.6
W	Ref	0.528	2	387	5905	1.750	6.7
	E8	0.471	3	348	4638	1.340	3.5

Table 10.
Mean values of engine and/or vehicle operating parameters obtained during the W and C sequences.

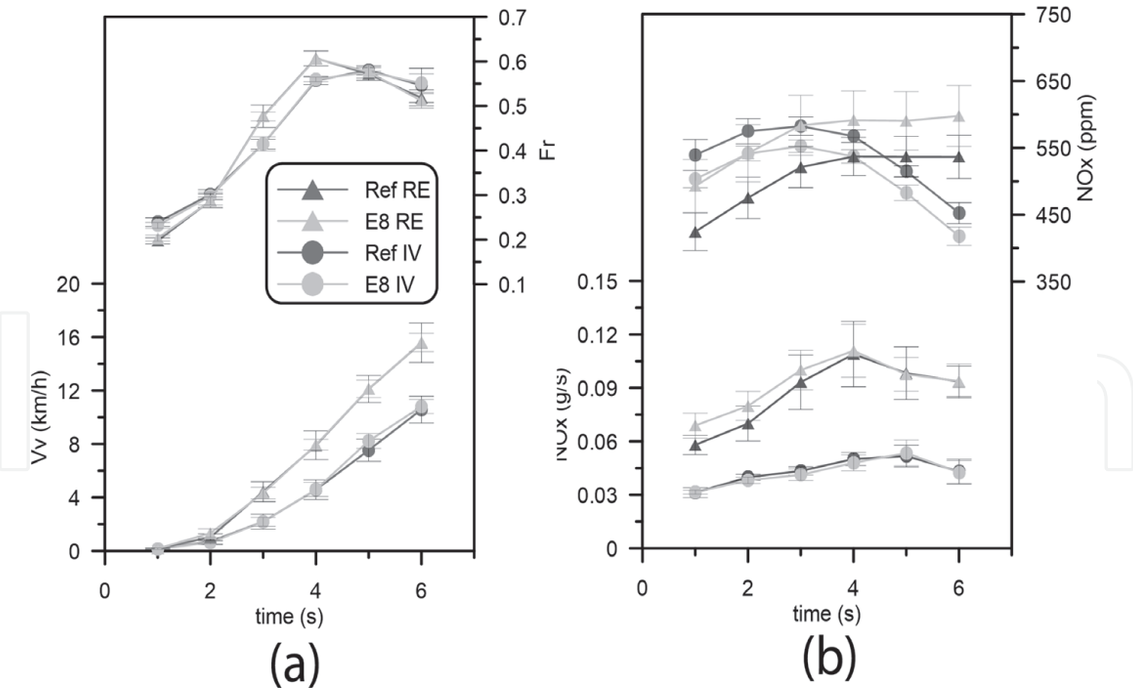

Figure 15.
Relative fuel-air ratio (Fr) and vehicle velocity (Vv) profiles (a) and NOx concentration and mass flow rate profiles (b).

Low NOx concentration produced by the E8 fuel blend when the IV bus was tested at Ciudad Real city, can be explained as follows: the higher enthalpy of vaporization and its cooling effect, combined with the lower oxygen availability at altitude, lead to a decrease in NOx concentration. This occurred even when the engine compression ratio of IV bus is higher than that of the RE bus. An opposite effect was registered the RE bus tests. The lower altitude of Seville leaded to a higher air oxygen availability during the combustion process that, together with the oxygen content of E8 blend, produced an increase of NOx concentration. This occurred even the lower engine compression ratio of the RE bus and the higher enthalpy of vaporization of E8 fuel blend both compared to the IV bus and the diesel fuel respectively.

Compared along the time analyzed and with each bus, NOx mass flow rates are similar between fuels. NOx mass flow rates differences between busses can be explained by the different engine displacement of busses. The RE engine is two liters larger than the IV engine. More displacement leads to more quantity of gas displaced by the engine.

Figure 16 shows time evolution of particle concentration emitted by busses with both fuels under the acceleration sequence. As shown in this figure, particle concentration evolution followed the time profiles of Fr (see **Figure 16a**).

Maximum particle concentration is reached around the 4th second as occurred with maximum Fr. Particle concentration increases proportionally respect to the Fr increase. As lower the oxygen concentration in the air as higher the particle concentration. Compared to diesel fuel, in both busses, particle concentration produced by E8 fuel blend is lower. Vehicles engines reproduce similar trend seen on the engine test bench. The lower quantity of aromatic compounds and the presence of molecular oxygen in E8 fuel blend lead to a cleaner combustion process and explain the obtained results.

3.4 Vehicle testing. Construction machinery

Average values of some characteristic parameters of the work done by the roller engine are listed in **Table 8**. These are indicative of the engine and/or vehicle

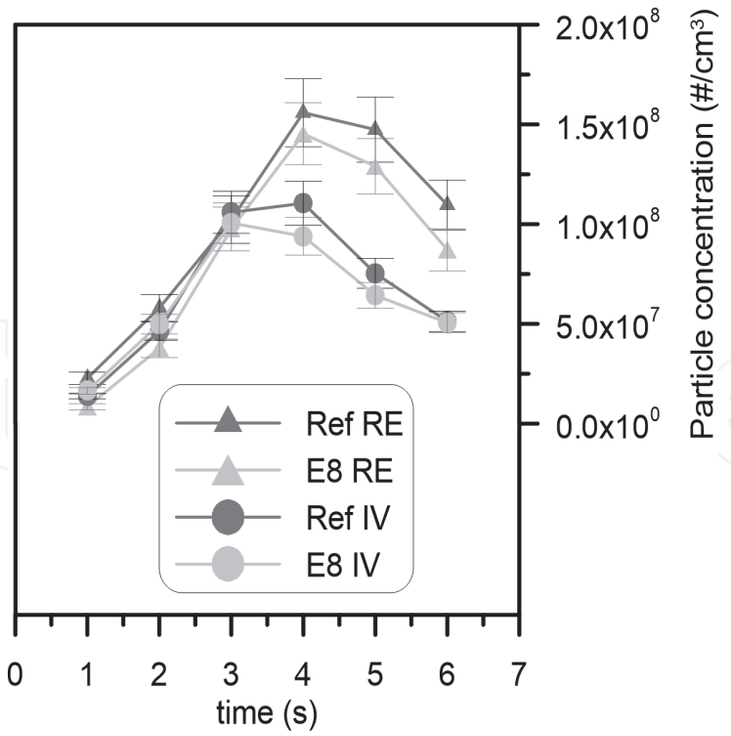

Figure 16.
Particle concentration profiles.

operation such as: relative fuel-air ratio (Fr), ambient temperature (T_{amb}, °C), exhaust gas temperature (T_g, °C), volumetric exhaust gas flow rate ($\dot{V}_g$, L/min), fuel mass flow rate ($\dot{m}_{fuel}$, g/s), and vehicle speed (v, km/h) for each operation sequence and fuel.

Figure 17 shows the relative fuel-air ratios, the smoke opacity and NOx concentration mean values registered during sequence C with both fuels. Important

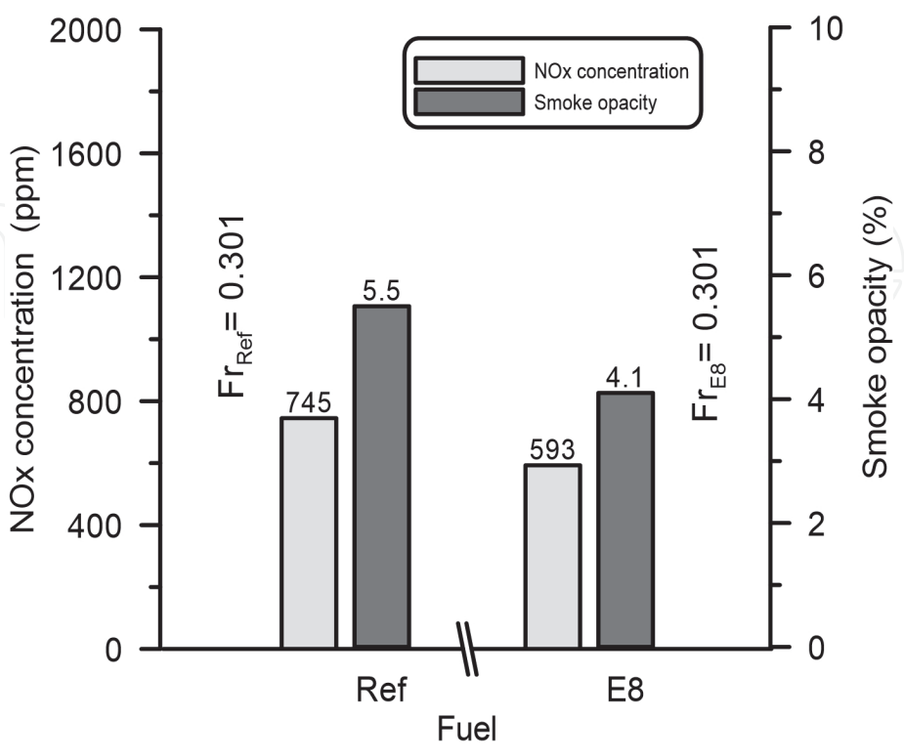

Figure 17.
Average values of relative fuel-air ratio, smoke opacity and NOx concentration from test fuels during the sequence C.

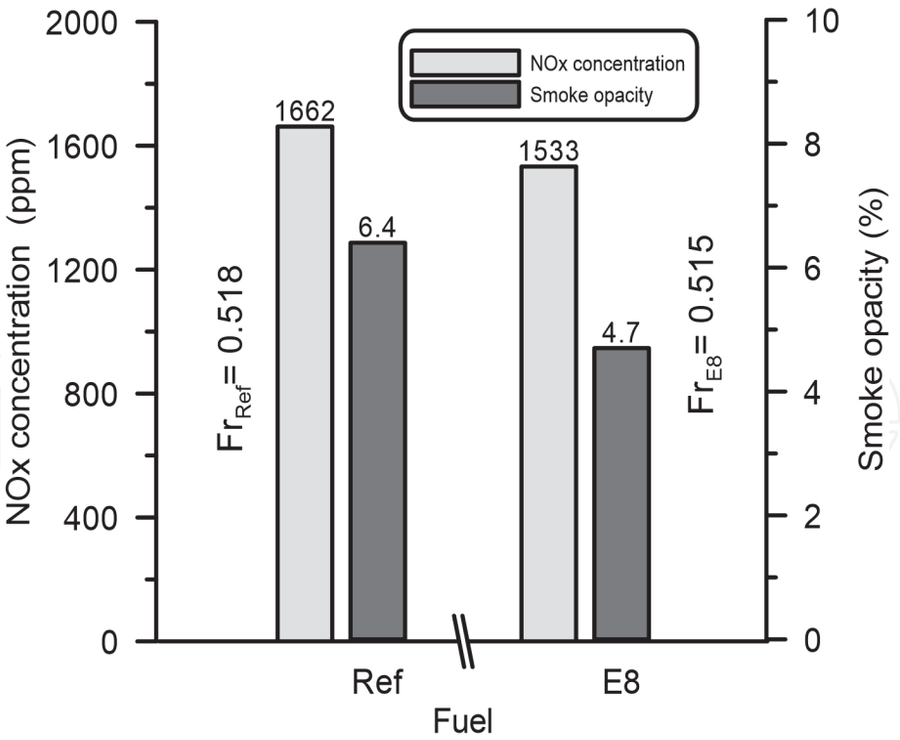

Figure 18.
Average values of relative fuel-air ratio, smoke opacity and NOx concentration from test fuels during the sequence W.

reductions of NOx concentration (20%) and smoke opacity (25%) was observed with E8 fuel. Smoke opacity reductions registered are comparable to results presented in [49].

Two factors contributed to provide reductions in NOx concentration higher than expected. First, the ambient temperature registered during the test with E8 fuel (9°C) lower than during the diesel tests. Second, machine velocity was 29% lower and thus the fuel consumption (as well as the exhaust gas flow) were lower (24%).

The average values of relative fuel-air ratios, smoke opacity and NOx concentration determined during the sequence W with both fuels are shown in **Figure 18**.

In this sequence NOx concentration and smoke opacity were reduced with E8 fuel blend 8% and 27% respectively. These decreases are in concordance with those presented in Ref.s [16, 47, 49]. During the test of this sequence, the ambient temperature was similar with both fuels. However, the E8 fuel consumption was 33% lower than the consumption of diesel fuel. This can be explained because the vibrating roller packed down harder ground when diesel fuel was used in comparison than when using E8. This difference, together with the lower machine velocity (16%) could partly explain the observed differences in opacity and NOx concentrations.

4. Strengths and weaknesses of the use of bioethanol mixed with diesel fuel

According to the results exposed in this chapter, most important strengths of the use of bioethanol blended with diesel fuel are the following:

- Molecular oxygen content of bioethanol is a key factor for reducing the emission of soot which is the main component of particulate matter emitted by diesel engines. Bioethanol molecular oxygen enables more complete combustion.

- Bioethanol, as linear chain alcohol, does not have aromatic compounds in its composition. In this sense, the addition of bioethanol to diesel fuel reduces the probability of soot nuclei formation in locally rich zones.

By the contrary, the use of bioethanol-diesel blends has several weaknesses:

- Limited miscibility reduces possibilities of using high percentages of bioethanol blended with diesel fuel. Low temperatures and high bioethanol concentration force the use of additives (such as biodiesel) to ensure the stability of bioethanol-diesel blends.

- Low lubricity is a key factor which negatively contributes on the lubrication of the injection systems and different engine parts. As occurred with miscibility, it is necessary the use of additives for improving lubricity properties of these blends.

- Bioethanol is highly hygroscopic. This forces to implement actions to avoid the water content increase of the blends. The water increase has double negative effect: decrease the miscibility of bioethanol-diesel blends and decrease their lubricity properties.

Other physicochemical properties of bioethanol can produce positive or negative effects on the engine operation when this alcohol is used blended with diesel fuel. However, the effects will depend on both the engine operating and ambient conditions. The high enthalpy of vaporization of bioethanol decreases the combustion process temperature, favoring lower NOx emissions under high engine load conditions but, under starting process or low engine load, this may provoke misfiring. Bioethanol has low cetane number that delay the start of combustion process which implies longer premixed phase of combustion. Also, bioethanol has low density and viscosity which can affect the fuel spray formation and its mixing with the inlet air. In this sense, the engine tuning should by adapted to fuel properties to maximize the benefits in terms of performance and emissions.

Author details

Octavio Armas Vergel[1*], Dolores Cárdenas[2], Reyes García-Contreras[1] and Carmen Mata[3]

1 Universidad de Castilla-La Mancha, Toledo, Spain

2 REPSOL, Madrid, Spain

3 Universidad de Castilla-La Mancha, Almadén, Spain

*Address all correspondence to: octavio.armas@uclm.es

References

[1] Agarwal AK. Biofuels (alcohols and biodiesel) applications as fuels for internal combustion engines. Progress in Energy and Combustion Science 2007; 33: 233–271. DOI: 10.1016/j.pecs.2006.08.003

[2] Ghadikolaei MA, Cheung Ch, Yung KF. Comparison between blended mode and fumigation mode on combustion, performance and emissions of a diesel engine fueled with ternary fuel (diesel-biodiesel-ethanol) based on engine speed. Journal of the Energy Institute 2019;92:1233-1250. DOI:10.1016/j.joei.2018.10.010

[3] Imran A, Varman M, Masjuki HH, Kalam MA. Review on alcohol fumigation on diesel engine: aviable alternative dual fuel technology for satisfactory engine performance and reduction of environment concerning emission, Renewable Sustainability Energy Review 2013;26:739-751. DOI: 10.1016/j.rser.2013.05.070

[4] Gomasta S, Mahla SK. An experimental investigation of ethanol blended diesel fuel on engine performance and emission of a diesel engine. International Journal of Emerging Technology 2012;3(1):74-79. ISSN (Online):2249-3255

[5] Can O, Çelikten I, Usta N. Effects of ethanol addition on performance and emissions of aturbocharged indirect injection Diesel engine running at different injection pressures. Energy Conversion and Management 2004;45: 2429-2440. DOI:10.1016/j.enconman.2003.11.024

[6] Abu-Qudais, M., Haddad,O., Qudaisat, M. The effect of alcohol fumigation on diesel engine performance and emissions. Energy Conversion & Management 2000;41: 389-399.DOI:10.1016/S0196-8904(99)00099-0

[7] Yao C, Cheung CS, Cheng C, Wang Y. Reduction of Smoke and NOx from Diesel Engines Using a Diesel/Methanol Compound Combustion System. Energy & Fuels 2007;21:686-691. DOI:10.1021/ef0602731

[8] Aakko P, Nylund NO, Westerholm M, Marjamäki M,Moisio M, Hillamo R, Mäkelä T. Emissions from Heavy-Duty Engine with and without After treatment Using Selected Biofuels. FISITA 2002 World Automotive Congress Proceedings, F02E195.

[9] Lapuerta M, Armas, O García-Contreras R. Effect of Ethanol on Blending Stability and Diesel Engine Emissions. Energy Fuels 2009;23:4343–4354. DOI:10.1021/ef900448m

[10] Pepiot-Desjardins P, Pistch H, Malhotra R, Kirby SR., Boehman AL. Structural group analysisfor soot reduction tendency of oxygenated fuels. Combustion and Flame 2008;154:191-205. DOI:10.1016/j.combustflame.2008.03.017

[11] Lapuerta M, Armas O, Herreros JM. Emissions from a diesel-bioethanol blends in anautomotive diesel engine. Fuel 2008;87:25-31. DOI:10.1016/j.fuel.2007.04.007

[12] Rakopoulos CD, Antonopoulos KA, Rakopoulos DC. Experimental heat release analysis and emissions of a HSDI diesel engine fuelled with ethanol-diesel fuel blends. Energy 2007;32: 1791-1808. DOI:10.1016/j.energy.2007.03.005

[13] Song C-L, Zhou Y-C, Huang R-J, Wang Y-Q. Influence of ethanol-diesel blended fuels on dieselexhaust emissions and mutagenic and genotoxic activities ofparticulate extracts. Journal ofHazardous Materials 2007;149: 355-363. DOI:10.1016/j.jhazmat.2007.03.088

[14] Giakoumis EG, Rakopoulos DC, Dimaratos AM, Rakopoulos D.C.

Exhaust emissions with ethanol or n-butanol diesel fuel blends during transient operation: Areview. Renewable and Sustainable Energy Reviews 2013;17:170-190. DOI:10.1016/j.rser.2012.09.017

[15] Ahmed I. Oxygenated Diesel: Emissions and Performance Characteristics of Ethanol-Diesel Blends in CI Engines. SAE 2001-01-2475.DOI: 10.4271/2001-01-2475

[16] Armas O, Cárdenas MD, Mata C. Smoke Opacity and NOx Emissions from a Bioethanol-Diesel Blend during Engine Transient Operation. SAE Technical Paper 2007-24-0131. DOI: 10.4271/2007-24-0131

[17] Armas O, García-Contreras R, Ramos Á. Pollutant emissions from engine starting with ethanol and butanol diesel blends. Fuel Processing Technology 2012;100:63-72. DOI: 10.1016/j.fuproc.2012.03.003

[18] Armas O, García-Contreras R, Ramos Á. Pollutant emissions from New European Driving Cycle with ethanol and butanol diesel blends. Fuel Processing Technology 2014;122:64–71. DOI:doi.org/10.1016/j.fuproc.2014.01.023

[19] Van Niekerk AS, Drew B, Larsen N, Kay PJ. Influence of blends of diesel and renewable fuels on compression ignition engine emissions over transient engine conditions. Applied Energy 2019;255: 113890. DOI:10.1016/j.apenergy.2019.113890

[20] Randazzo ML, Sodré JR. Exhaust emissions from a diesel powered vehicle fuelled by soybean biodiesel blends (B3–B20) with ethanol as an additive (B20E2–B20E5). Fuel 2011;90:98-103. DOI:10.1016/j.fuel.2010.09.010

[21] Mata C, Gómez A, Armas, O. The influence of ethanol-diesel blend on pollutant emissions from different bus fleets under acceleration transitions. Fuel 2017;209:322–328. DOI:10.1016/j.fuel.2017.08.018

[22] Kass M, Thomas J, Storey J, Domingo N, Wade J, Kenreck G. Emissions From a 5.9 Liter Diesel Engine Fueled With Ethanol Diesel Blends. SAE Technical Paper 2001-01-2018: DOI: 10.4271/2001-01-2018

[23] Armas O, Lapuerta O, Mata C, Pérez D. Online Emissions from a Vibrating Roller Using an Ethanol-Diesel Blend during a Railway Construction. Energy & Fuels 2009;23:2989–2996. DOI: 10.1021/ef900148c

[24] Merrit PM, Ulmet V, McCormick RL, Mitchell WE, Baumgard KJ. Regulated and Unregulated Exhaust Emissions Comparison for Three Tier II Non-Road diesel Engines Operating on Ethanol-Diesel Blends. SAE Paper 2005-01-2193. DOI:10.4271/2005-01-2193

[25] Hansen AC, Zhang Q, Lyne PWL. Ethanol–diesel fuel blends–a review. Bioresource Technology 2005;96:277–285. DOI:10.1016/j.biortech.2004.04.007

[26] Lapuerta, M., Armas, O., García-Contreras, R. Stability of diesel–bioethanol blends for use in diesel engines. Fuel 2007;86:1351–1357. DOI: 10.1016/j.fuel.2006.11.042

[27] Waterland LR, Venkates, S, Unnash S. Safety and Performance Assessment of Ethanol/Diesel Blends (E-Diesel). NREL/SR 2003;540:34817.

[28] Huang J, Wang Y, Li S, Roskilly AP, Yu H, Li H. Experimental investigation on the performance and emissions of a diesel engine fuelled with ethanol-diesel blends. Applied Thermal Engineering 2009;29:2484-2490. DOI:10.1016/j.applthermaleng.2008.12.016

[29] Di Y, Cheung CS, Huang Z. Experimental study on particulate

emission of a diesel engine fueled with blended ethanol-dodecanol-diesel. Journal of Aerosol Science 2009;40:101-112. DOI:doi.org/10.1016/j.jaerosci.2008.09.004

[30] Makareviciene V, Sendzikiene E, Janulis P. Solubility of multicomponent biodiesel fuel systems. Bioresource Technology 2005;96:611-616. DOI: 10.1016/j.biortech.2004.06.007

[31] Lei J, Shen L, Bi Y, Chen H. A novel emulsifier for ethanol–diesel blends and its effect on performance and emissions of diesel engine. Fuel 2012;93: 305-311. DOI:10.1016/j.fuel.2011.06.013

[32] McCormick RL, Parish R. Advanced Petroleum Based Fuels Program and Renewable Diesel Program. Milestone Report: Technical Barriers to the Use of Ethanol in Diesel Fuel. NREL/MP 2001;-540:32674.

[33] Kwachareon P, Luengnaruemitchai A, Jain-In S. Solubility of a diesel-biodiesel-ethanol blend, its fuel properties, and its emission characteristics from diesel engine. Fuel 2007;86:1053-1061. DOI:10.1016/j.fuel.2006.09.034

[34] Pires de Oliveira I, Lima Caires AR, Baskar K, Ponnusamyd S, Lakshmanan P, Veerappan V. Biodiesel as an additive for diesel-ethanol (diesohol) blend: physical-chemical parameters and origin of the fuels' miscibility. Fuel 2020;263:116753. DOI:10.1016/j.fuel.2019.116753

[35] Fernando S, Hanna M. Development of a Novel Biofuel Blend Using Ethanol-Biodiesel-Diesel Microemulsions: EB-Diesel. Energy & Fuels 2004; 18:1695-1703. DOI:10.1021/ef049865e

[36] Lapuerta M, García-Contreras R, Agudelo JR. Lubricity of Ethanol-Biodiesel-Diesel Fuel Blends. Energy & Fuels 2010;24:1374–1379. DOI:10.1021/ef901082k

[37] Armas O, Mata C, Martínez-Martínez S. Effect of an ethanol–diesel blend on a common-rail injection system. International Journal of Engine Research 2012;13(5):417–428. DOI: 10.1177/1468087412438472

[38] McCormick RL and Parish R. Technical barriers to the use of ethanol in diesel fuel. National Renewable Energy Laboratory, Golden, Colorado, http://www.afdc.energy.gov/afdc/pdfs/barriers_eDiesel.pdf (2001).

[39] Mickevičius T, Slavinskas S, Kreivaitis R. Effect of ethanol on performance and durability of a diesel common rail high pressure fuel pump. Transport 2016;31(6). DOI: 10.3846/16484142.2015.1058292

[40] Yahuza I, Dandakouta H. A Performance Review of Ethanol-Diesel Blended Fuel Samples in Compression-Ignition Engine. Journal of Chemical Engineering & Process Technology 2015;6(5). DOI: 10.4172/2157-7048.1000256

[41] Chandler K, Whalen M, Westhoven J. Final Results From The State Of Ohio Ethanol-Fueled Light-Duty Fleet Deployment Project. SAE Technical Paper 982531. DOI: 10.4271/982531

[42] Kane E, Huang Y, Mehta D, Frey CM, Tillerson Z, Chavis S. Refinement of a Dedicated E85 1999 Silverado with Emphasis on Cold Start and Cold Drivability. SAE Technical Paper 2001-01-0679. DOI: 10.4271/2001-01-0679

[43] Macian V, Bermúdez V, Payri R, Gimeno J. New technique for determination of internal geometry of a diesel nozzle with use of silicone methodology. Experimental Techniques 2003;27(2):39–43. DOI: 10.1111/j.1747-1567.2003.tb00107.x

[44] Armas O, Lapuerta M, Mata C. Methodology for the analysis of pollutant emissions from a city bus.

Measurement Science and Technology 2012;23:045302. DOI: 10.1088/0957-0233/23/4/045302

[45] Can Ö, Celikten I, Usta N. Effects of ethanol addition on performances and emissions of a turbocharged indirect injection Diesel engine running at different injection pressures. Energy Conversion and Management 2004;45: 2429-2440. DOI:10.1016/j.enconman.2003.11.024

[46] De-gang L, Huang Z, Lu X, Zhang W, Yang, J. Physico-chemical properties of ethanol-diesel blend fuel and its effect on performance and emissions of diesel engines. Renewable Energy 2005; 30:967-976. DOI: 10.1016/j.renene.2004.07.010

[47] Xing-cai L, Jian-guang Y, Wu-gao Z, Zhen H. Effect of cetane number improver on heat release rate emissions of high speed diesel engine fuelled with ethanol-diesel blend fuel. Fuel 2004;83: 2013-2020. DOI: 10.1016/j.fuel.2004.05.003.

[48] Mohanmmadi A, Ishiyama T, Kawanabe H, Horibe N. An optimal usage of recent combustion control Technologies for DI diesel engine operating on ethanol blended fuels. SAE paper 2004-01- 1886. DOI: 10.4271/2004-01-1866.

[49] Subramanian KA, Singal SK, Saxena M, Singhal S. Utilization of liquid biofuels in automotive diesel engine: An Indian perspective. Biomass and Bioenergy 2005;29:65-72. DOI: 10.1016/j.biombioe.2005.02.001